Technical Design Report

Everett Wind Energy Team - EWET

Washington State University-Everett with Everett Community College

11/23/2021~5/6/2022

Team Members

Steven Fordham WSU Electrical Team Lead	Steven Fordham WSU Turbine Controls	Steven Fordham WSU Electrical Design	Tamara Roberson WSU Load Controls
Boris Gindlin WSU Electrical Design	Boris Gindlin WSU Generator Design	Boris Gindlin WSU Load Design	James Garfield EvCC MakerPlot HMI Research
Dan Gilles WSU Mechanical Team Lead	Dan Gilles WSU Aerodynamics	Ryan Phillips WSU Foundation Design	Eric Martin EvCC Project Development
Taylor Funk WSU-Everett Content Creation and Digital Outreach	Quinn Yackulic EvCC Project Development	Taylor Funk WSU-Everett Digital Content Creator	Taylor Funk WSU-Everett Social Media Manager

Advisors

Dr. Gordon Taub WSU-Everett Principle Investigator	Joe Graber EvCC Co-PI	Jacob Murray WSU Co-PI	Xie Shuzheng WSU Co-PI

Executive Summary

This report summarizes collective knowledge and documents to date practical results in the field of wind power generation, achieved by the WSU-EvCC cross-institutional team. Additionally, a portion of this work concerning electrical engineering, signify a senior capstone project achievement for the WSU electrical engineering team. Current academic year's success recognizes and builds on the previous year's wind energy team's extensive research and is grateful for their intellectual legacy. This year, the team has taken a top-down approach to research and development of the prototype. It was decided to avoid extensive fundamental research and study of competitors' achievements. Design priority was given to the commercially available components based on a trial-and-error approach. This permitted relative freedom from the burdens of predisposition to operate in the wake of someone else's success, allowing more experimental courage and satisfaction with the accomplishments. This year, the team has returned to the traditional horizontal-axis wind turbine design with autonomous pitch, yaw, and load control. Although autonomous yaw control was beyond the CWC requirements, the design experience was determined to be beneficial to the achievements within the scope of the senior capstone project, and perhaps future teams' research. The electrical team has expanded on the previous year's turbine and load control component ideas and developed its own robust approach to power management, voltage regulation, and generator selection. The mechanical team had more work cut out for them due to the previous year's work on a vertical-axis turbine having very few design solutions that were applicable for a horizontal-axis design. After initial experiments and conceptual deliberation, the control team has settled on selecting the rotational speed of the machine as the primary pitch control input and wind speed as the primary load control input, implementing separate controllers for each device connected via a communication bus. Additionally, beyond the CWC requirements scope, some team members' time was dedicated to the development of the HMI, data acquisition, and live power output monitoring systems, this was done with consideration for broader wind farm project development. For this purpose, MakerPlot software was chosen, and a suitable application was developed, however because of limited competence in this field of work and limited human resources it was not integrated into the final design. The immediate state of the prototype and the project progression is determined satisfactory. The team was able to achieve its selected objectives in control of the turbine and power generation. Work is continuing to finalize turbine-load communication, final blade, and foundation design along with revisions to the pitch actuator mechanism.

1. Introduction

Our team has picked the horizontal axis turbine because we wanted a more conservative approach in wing energy generation, compared to the previous year. The team's main goal this year was to come up with a functional generation system, that could create a baseline for future experiments and designs. The advantage of the horizontal axis was in the fact that its design concept has been well researched, and a wealth of information is available on the topic. This way more time could be spent, trying out different working designs in the attempt to develop our own. Nevertheless, a

fair share of challenges had to be overcome by the team. One of the critical concerns this year is involving the weight and balancing of the prototype since this year's competition has an offshore theme and the turbine structure will need to reside on the simulated ocean floor. Because of this reason, vibration, weight, balancing, and aerodynamics became very important to design criteria. To maintain minimal weight and have adequate aerodynamical properties, there was no other option but to use the 3D printing technology. This insured lightweight of the structural elements, fast prototype turnaround, and allowed to model and produce complex aerodynamic shapes of the turbine housing structure. Another set of technical challenges was due to the active pitch control design, initial attempts to control the actual degree of the pitch did not come to fruition, because the team did not find a solution to accurately control the position of the blades. This led to a more elegant idea of the "speed control", where the turbine control system is monitoring the rate of speed change and makes decisions to pitch up, pitch down, or to do nothing if it is at the target speed. Active yaw control was mostly for the team's own research to develop an understanding of how larger wind turbines that do not have passive yaw control are positioned into the wind. The original load control idea was to have a continuous load control, the team has settled for discrete control because resistive load range was unknown at the beginning of the design process and since the CWC rules wind speeds are also discreet a simpler, wind sensor dependent load control solution was adopted. Generator selection just happened to naturally work out in terms of weight distribution, because its stack could be evenly split over the center of the pole, this has proven to be one of the benefits of axial flux permanent magnet (AFPM) machines, compared to permanent magnet brushless machines that need counterbalancing. An additional feature of the AFPM was the fact that its fundamental geometrical design properties provide for a relatively large hollow center in its stator. This gives significant flexibility to the pitch actuator design approach, which our mechanical team has successfully implemented using a linear actuator mechanism powered by DC/Stepper motor.

2. Design Objectives and Components

The objective of our turbine design team was to create a turbine that performed well in the CWC test environment. The turbine had to fit within the bounding box shown in Figure 1. The bounding box is a 45 cm cube mounted on a 15 cm diameter cylinder which extends downwards to the underwater foundation attachment resting on the 24x25x15 cm^3 cube of water immersed sand. The turbine blades need to be completely enclosed in the cube. The turbine was supposed to start at the lowest wind speed possible, then produce power of varying levels until wind speeds of 11 m/s and respond to the load disconnect scenario in a controlled manner. All turbine components were to be designed to withstand wind speeds of 22 m/s. The electrical system needed to work with an out-of-box motor to be used as a generator. The motor produced AC power which needed to be converted to usable DC power. A system to adjust the resistance on the circuit to maintain optimal power output during the variable conditions needed to be designed. Finally, a control system needed to be designed to adjust pitch based on the rotational speed of the turbine and maintain maximum torque generated from the wind.

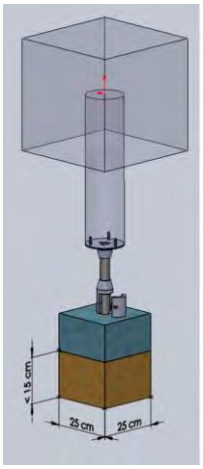

Figure 1. Design constraints

3. Electrical Design and Controls

3.1 Introduction

In the small-scale turbine design, it is critical to identify the type of generator that would be used through the design process because mechanical designs and modeling are time consuming and constrained by the academic year's available man hours. It is important to limit complete change of design course to one or two instances and even that is only affordable at the initial stage of the design. The team did not have a ready generator solution from previous project and had no practical experience in assessing the scale or the needed parameters in selecting the generator for such a miniature design. The only notion that was passed down from previous team was the understanding of the electrical motor KV rating and importance of minimizing cogging torque at cut in speed. Thus, these became the starting point parameters in the generator selection. The team has encountered several challenges in the power electronics selection process. Ideas have been tried and discarded, some because the component selection process was not taking into account the component's self-power demand, others because the nature of the component's operation was not fundamentally understood. In some instances, where a solution was not found by a direct approach, like in voltage regulation attempts, the team has paused on that front and shifted attention to better-understood sections of the design, allowing for continuous progress. This approach proved to be very effective, and more elegant and natural solutions were found as a result.

3.2 Generator and Load

Faraday's Law indicates that *"Any change in the magnetic environment of a coil of wire will cause a voltage (emf) to be induced in the coil".* Formulation (1) demonstrates the physical relationship described by Faraday using mathematical interpretation.

$$Emf = -N\frac{\Delta\phi}{\Delta t} (1)$$

Where N represents the number of turns in the coil, $\Delta\boldsymbol{\Phi}$ represents a change in magnetic flux over time, Δt - change in time. Magnetic flux is given by formulation (2).

$$\phi = BA\sin\theta\ (2)$$

Were B represents the magnetic field, produced by opposing permanent magnets of the rotors, A represents the area of the coiled wire in the stator and θ represents the angle between the coil area plane and the magnetic field and since the coil area and the magnetic field are orthogonal to each other in the AFPMG, formulation (2) can be restated as

$$\phi = BA\ (3)$$

According to Lenz's law, the negative sign of (1) indicates that the current produced by the change in magnetic flux creates its own magnetic field that opposes the change in flux that produced it. When applying this notion to a generator this indicates that the current induced in the generator coils will provide an opposing force to the one that is responsible for the rotation of the generator shaft. Since the force is rotational it could be restated in terms of opposing torque τ(G) and compared against aerodynamic torque τ(W) extracted from the wind.

$$\tau_W = \frac{P_w}{\omega_{rotor}} = \frac{\rho\pi R^3 c_p(\lambda,\theta)V_W^2}{2\lambda}\ (4)$$

Where P_W, in watts, is the power available in the wind and is given by (5), ω_{rotor} is the rotational speed in (rad/s), ρ is the air density in (kg / m3),

$$P_w = \frac{\rho \pi R^2 c_p(\lambda, \theta) V_W^2}{2} \quad (5)$$

C_p is the power coefficient expressed as a function of the tip speed ratio and pitch angle and is given by (6 and 7)

$$\tau_R = \frac{P_w \times c_p}{\omega_{rotor}} c_p(\lambda, \theta) = .22\left(\frac{116}{\lambda_i} - .040 - 5\right) e^{\frac{-12.5}{\lambda_i}} \quad (6)$$

$$\lambda_i = \frac{1}{\left[\frac{1}{\lambda + .080} - \frac{.035}{\theta^3 + 1}\right]} \quad (7)$$

R is the wind turbine rotor radius in (m), V_w is the wind velocity in (m/s), and λ is the tip speed ratio (TSR) given by (8).

$$\lambda = \frac{R\omega_{rotor}}{V_w} \quad (8)$$

It could be further inferred that wind turbine operation could be imagined as a system of two opposing torques τ_w and τ_G whenever torques are equal the system is in equilibrium and is generating constant power. Any time τ_w changes in response to change in V_w, (*for the experimental environment ρ is assumed constant*) there exists a new equilibrium state of τ_w and τ_G torques. Simply put, anytime V_w increases it creates conditions for a new and greater power equilibrium state, this means the resistance of the load could be decreased, which will increase the current flow, and thus more power could be extracted from the wind.

The KV rating of the generator is responsible for predicting the magnitude of the generated voltage as a function of the rotor speed. In the wind turbine controls it is sometimes important to maintain a relatively low rotational speed and at the same time maintain a voltage magnitude that is high enough to keep the microcontroller active (10) and (11) show this relationship.

$$KV_{rating} = \frac{1}{slope\ of\ the\ \left(\frac{voltage}{rotor\ speed}\right)} \quad (10)$$

$$V = \frac{RPM}{KV_{rating}} \quad (11)$$

Cogging torque is a magnetic interaction between the iron teeth of the stator and magnets of the rotor in a brushless DC motor for instance. The team did not know how to assess the magnitude of such torque and its effect on the cut-in speed of the future turbine so naturally, attempts were made to find a motor with little to no cogging torque. This led to the discovery of the axial flux permanent magnet motor (AFPMM) which could be used as a three-phase DC generator if coupled with a three-phase full rectifier circuit. Figure 1 shows the single rotor and the stator of the 12 pole 9 coil AFPMG used in the prototype. A set of two motors were purchased for initial evaluation of the KV rating. Using a dynamometer, it was experimentally determined that

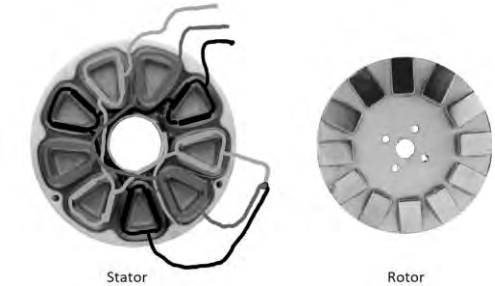

Figure 2. AFPMG rotor and stator

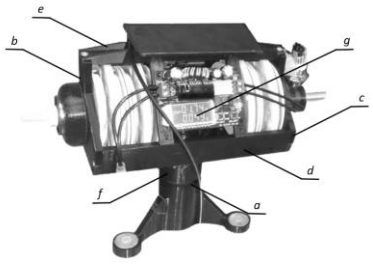

Figure 3. Housing assembly

the KV rating of the single motor was 96. This was very low comparing to all other available options that also had the appropriate dimensional scale. Evaluating the mechanical construction of the motor's design, it was observed that stacking these motors onto a single axle would be relatively simple. Once the team recognized the flexibility in the connection schemes, the ability to reduce the KV rating to 24 by stacking motors on the single axle, and the virtual absence of cogging torque in this design, two more motors were immediately ordered. Figure 3 demonstrates the midterm version of the generator design. The housing assembly consists of five main parts: (b and c) front and back bearing supports, (d) housing block, (e) stabilizer bar, and (f) yaw pivot assembly.

The drivetrain assembly is shown in Figure 4. is composed of the central axle (a) that connects four pairs of inline rotors (b and c) and two pairs of stators (d and e). The stators are supported by the housing assembly and are independent of the rotation of the rotor assembly. Connected to each pair of stators are housing assemblies that contain two pairs of internally connected full-bridge rectifiers potted in epoxy. Once the generator selection was settled on, mechanical design and power electronics work began. Figure 5 shows the systems power distribution of the most recent design review.

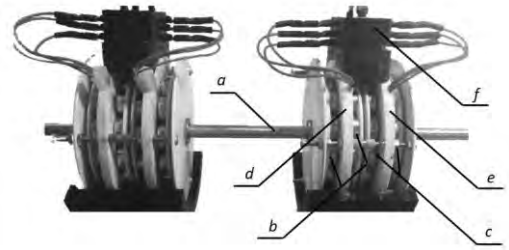

Figure 4. Drivetrain assembly

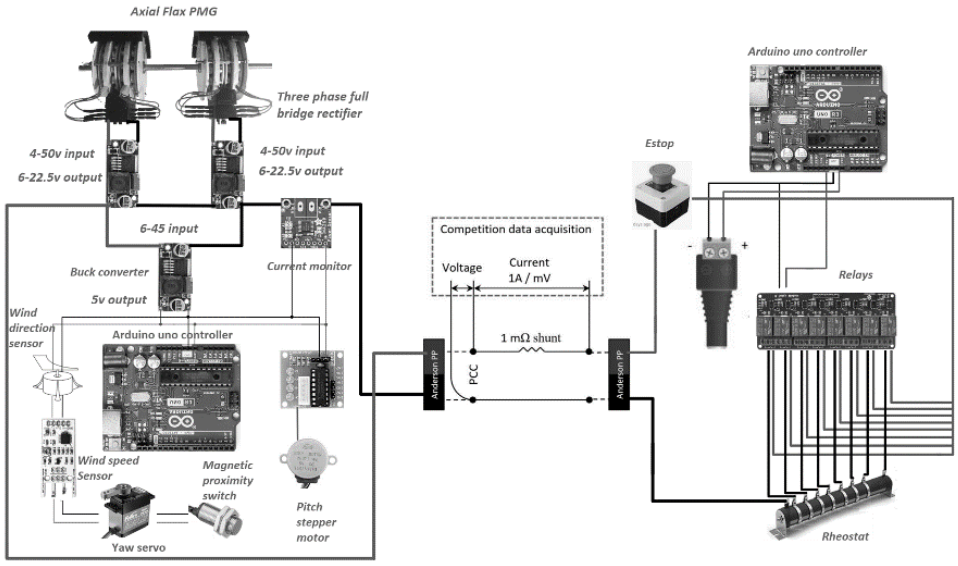

Figure 5. Pictorial schematic of the turbine's control and load power distribution

The load chosen is constructed of a 200W variable resistor with coils and contacts throughout to select the desired resistance for the appropriate wind speed and scenario. Supplemental resistance was needed for the lower wind speed and lower load conditions, so additional resistors are

combined in series to acquire these values. The resistance values used in the load box vary from 45 ohms up to 420 ohms. A relay bank controlled by a separate Arduino from the turbine is used to select the load by closing the contacts on the desired resistor value. The Arduino is receiving commands from the turbine through an optically isolated TX and RX line. This Arduino will send commands to the turbine if a manual shutdown is required.

3.3 Control Theory

The pitch control scheme is made up of a methodology called Fuzzy Logic. The tachometer measures the RPM of the turbine and then the controller determines how far away the current RPM is from the desired RPM of the turbine. The previous RPM record is also taken into consideration when determining whether to make a pitch adjustment or not. If the turbine is rotating too slowly but is speeding up, the algorithm will wait for another cycle to see if the pitch has continued to increase the RPM, and if not, it will then make an appropriate adjustment based on how far away from the desired RPM it is. If the turbine RPM is within acceptable bounds to the desired RPM, then no adjustments will be made.

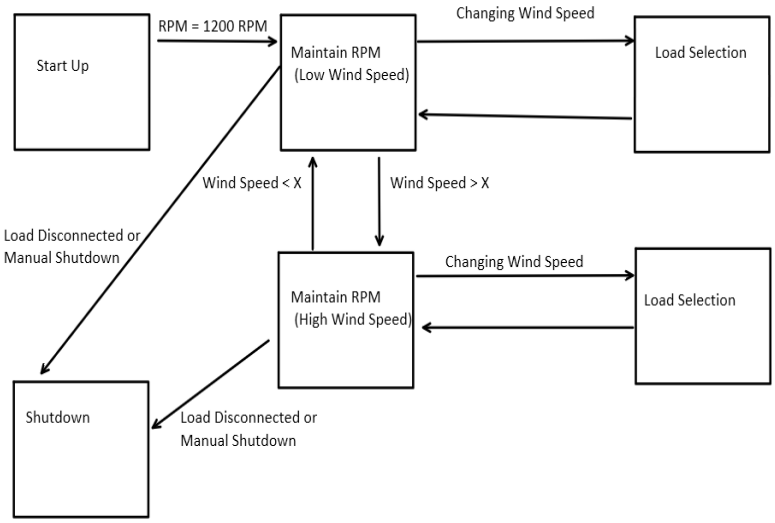

Figure 6. Canonical Control Model

The tachometer utilizes a hall effect sensor that counts the number of pulses it receives, which happens once per revolution, calculated the period it takes for 20 revolutions to occur, and determines the RPM from this math. There is a time-out scenario where if 20 revolutions have not been completed in 5 seconds the loop will break and the RPM will still be calculated, just with less accuracy because the time period over fewer revolutions will be averaged.

A current sensor must be used to determine if the load has been disconnected from the turbine. An ADA260 module communicates with the Arduino via an I2C connection. When the load goes above 50 mA the load is detected, and any drop below that will trigger the pitch to adjust to slow the blades down to a stop. The minimum load expected at a wind speed of 5 m/s is around 80 mA so this is not something that could be accidentally tripped.

The wind speed sensor determines the wind speed utilizing the “hot wire” method. This method heats up a wire and as the wind passes by, it cools the wire off changing its resistance and the voltage across it. The voltage is read by the Arduino and then the Arduino can determine the wind speed the sensor is experiencing.

Delays are important for the pitch control system because it takes some time for the system to stabilize and the RPM to cease any fluctuations. The problem with using the built-in delay functions is that the Arduino cannot do anything else while this is happening. A modified delay function was made so that crucial measurements can be made in this idle time to allow action to be taken if something doesn't look right. The current is monitored so if the load is disconnected, the turbine can immediately begin slowing down to prevent over-speeding the turbine and damaging both the physical and electrical components.

Currently, the pitch control mechanism is adjusted by a stepper motor, but through testing it has been noticed that the stepper motor has a few flaws, being it is slow, and it draws a lot of current. The stepper motor takes more than 20 seconds to move from one extreme pitch setting to the other. This affects the RPM when the load is disconnected because the elimination of torque due to the load results in the turbine increasing by several hundred RPM during disconnects. With faster pitching speeds, this RPM overshoot can be minimized. Because the stepper motor draws around 300 mA the added load during pitch adjustments slows the blades down and results in more time needed for the RPM to stabilize after pitch adjustments are made. It is being considered to change to a DC motor with a gearbox and H-bridge configuration which alleviates both concerns in preliminary testing, with the current selection having more speed while also drawing less current.

3.4 Voltage Regulation Description

The voltage regulation system consists of four axial flux motors tied in series after their respective voltages have been rectified. This allows for a high KV rating which is important for the low RPM operation of the Arduino. Two adjustable buck convertors are each attached to two rectifier outputs in series, limited to 22.5 V. When these two buck converters are connected in series the system total voltage is limited to 45 V. Two buck converters connected in series are needed because each is rated for 52 V. allowing for a maximum turbine voltage of 104 V which is achieved at around 2400 RPM or twice the 1200 RPM normal operational speed of the turbine. The initial intent was to achieve a high voltage quickly to run the Arduino at low RPMs and sustain it for the manual and emergency stop scenarios so that the turbine could automatically restart.

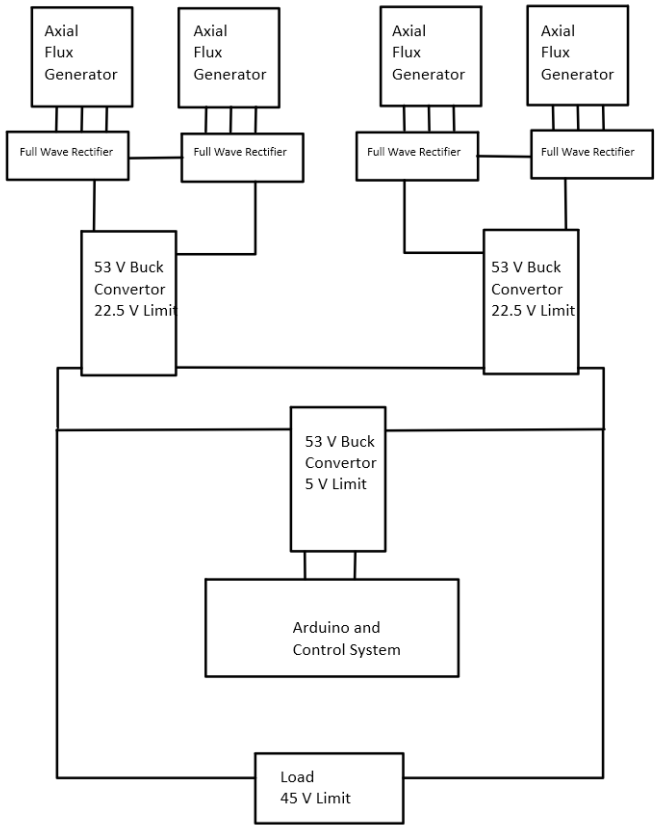

Figure 7: Voltage Regulation Diagram

Unfortunately, through testing it was discovered that each of the buck converters requires a minimum of 4.5V to operate, which now brings the minimum operating voltage to 9V instead of the 5V that the Arduino needs to say alive. Applying the KV rating formula from (10) gives 216 RPM as the minimum rotational speed for the turbine's control system to operate. This would require the normal operational speed of the turbine to go up by 960 RPM to 2160 RPM, this is according to CWC 10% of the maximum speed requirement during the load-disconnect shutdown procedure. Because during the emergency shutdown it takes time for the system to respond to the load being disconnected, there exists a time where RPM continues to rise. Having only 240 RPM buffer before buck converters' operational limit is surpassed by over-voltage, brings a self-restart operation of the turbine to the unpredictable operation conditions, where buck converter failure is very likely. From observation, the system can surpass the 240 RPM buffer zone faster than the control system can respond to slow itself down. At this time, the team was not able to find a solution for this problem, and the turbine is designed to be manually restarted after an emergency stop. A faster pitch control system is being designed, using a DC motor, gearbox, and limit switches to prevent overtravel. More tests are needed to determine if the new pitch control scenario will deliver the self-restart capability.

3.5 Software Development

A lot of adjustments and improvements have been made to the pitch control algorithm. At first, there were 5 choices the program could make to adjust the pitch: no adjustment and small/big adjustment to make the blades go faster/slower. Later it was observed that if the blades were accelerating towards the desired RPM, there may not need to be any adjustment made. The pitch adjustment motor used also requires power to use, and so with every pitch adjustment, not only is there a delay required due to the change in aerodynamics, but the additional load that the motor requires will slow the turbine down as well, which may need additional time to allow for RPM stabilization. As the wind speed increases, because there is more power in the wind, the turbine reacts more quickly to pitch changes, and so the delay times must be shortened as wind speed increases. The turbine is also more sensitive to pitch changes at high wind speeds and RPM, and so the adjustments made are smaller as the wind speed increases. If the turbine is trying to supply more power than it can extract from the wind, which would cause the RPM to drop due to blade stall. The blades will pitch back to a previous setting to try and reduce or save the stall condition if too many "large pitch adjustment faster" conditions occur consecutively. While the delay functions built into the Arduino software work well, the current cannot be measured during this delay time, and so if the load is disconnected it could be up to three seconds before it is noticed by the software, which could cause the blades to overspeed. A modified delay function had to be created so that sufficient delays could still be implemented, and the current could be checked in case of a disconnect, immediately pitching the blades back and breaking the turbine.

Wind speed measurement has been more difficult than it was anticipated. The Rev C wind speed sensor is very sensitive at low wind speeds, but at high wind speeds the voltage it sends out only varies by a couple of hundredths of a volt per meter per second of wind. This made it challenging to know exactly what the wind speed was so a lot of measurements are taken and averaged and then compared with previous wind speed measurements to try and verify if the wind speed is constant or it is changing to a higher or lower speed.

4. Mechanical Design

The EWET Mechanical Team chose the horizontal axis wind turbine early in the Fall Semester for the reasons of simplicity. While starting with essentially a blank slate, the physical structure of the turbine was divided up into sections: The foundation, the tower, the nacelle, yaw control, pitch control and the blades. Initial discussions among team members helped to guide our design process. The foundation would most likely implement augers to anchor to the sand. The yaw system was chosen to be active to avoid the extra drag from a tail fin. The brake system early on was discussed as a disc brake system but could implement pitch control assisted braking. The nacelle would be located directly behind the rotor. The following subsections of the design report will discuss details of the final design that will be presented for the 2022 CWC competition.

Figure 8: Angle view of EWET's final prototype wind turbine for the 2022 CWC competition.

4.1 Yaw

The yaw system for the wind turbine has only one task for one brief moment. When the wind turbine is placed in the tunnel, it must yaw into the direction of the wind just once and maintain that position for the duration of the test. The options of having a passive or an active system were both discussed. Since the 2022 competition had the additional foundation requirement, the consideration for reduced drag was made. A passive yaw system would have an additional tail fin which would have an increased drag effect. This additional force would have to be accounted for in the foundation. For this reason, an active yaw system was designed. This design used the combination of two features; a double thrust bearing system and a spur gear combination with a 7:1 ratio.

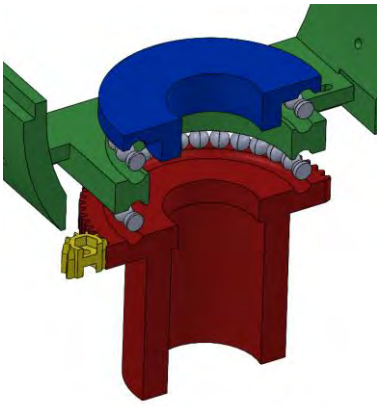

Figure 9: Yaw mechanism section view

The double thrust bearing system was completely 3D printed due to its complex nature. The large diameter of the track for the ball bearings was to ensure stability. The spur gear arrangement was implemented merely for the use of a small, low power drawing, continuous servo motor. The 7:1 ratio would ensure the servo would have increased torque capability to adjust the nacelle. Testing in a wind tunnel proved that the servo would be able to hold the wind turbine steady up to 13 m/s. The bottom of the yaw system connects directly to the top of the tower assembly.

4.2 Pitch

It became clear early on through conversations with the electrical engineering team that the goal for this turbine would be to have a target RPM as opposed to a target tip-speed ratio. This meant that that the wind turbine would have to have an active pitch controlling mechanism to account for changes in the wind. A large amount of effort was put into the design of a pitch mechanism. Inspiration was drawn from internet searches and team input. The final choice would be a system utilizing a hollow shaft with a smaller pitch controlling rod going through, that would change the pitch of the blades Figure 10. This system could further be broken down into two parts, front and

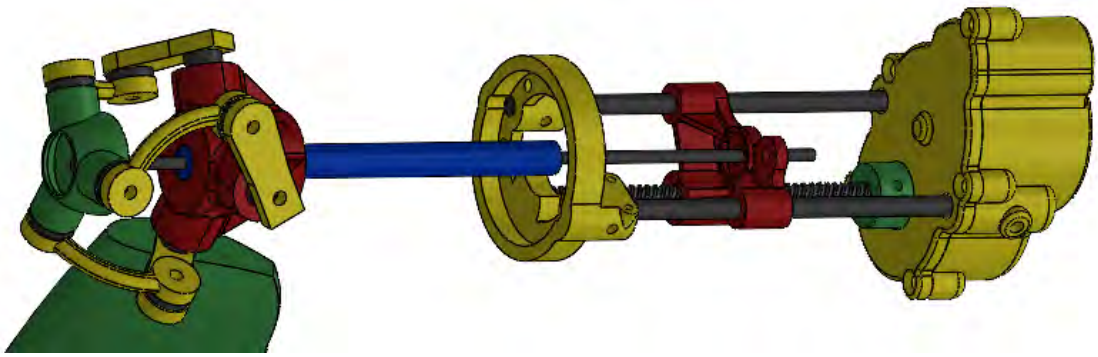

Figure 10: Total pitch mechanism with nacelle removed to show the interaction between the front and rear mechanisms.

rear.

At the front, integrated into the rotor, the pitch controlling rod moves a central piece that uses leverage to twist the three blades simultaneously. On the rear end, where the pitch controlling rod passes through the axle on the back of the nacelle, a linear actuator would precisely change the position of the pitch controlling rod to control the pitch.

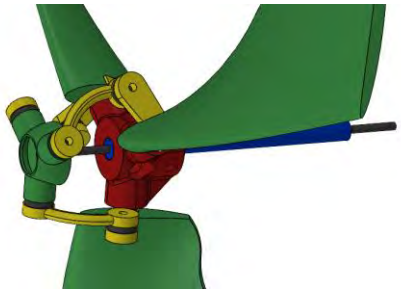

Figure 11: Front of pitch mechanism

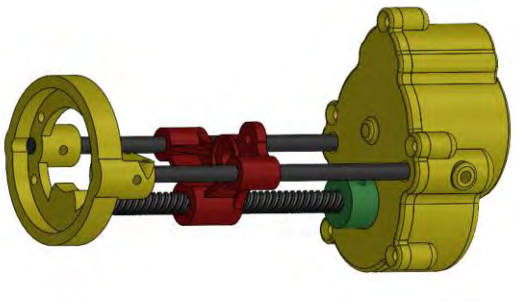

Figure 12: Rear section of pitch mechanism

As seen in figure 11 each blade has a lever arm attached which is connected with another member to a central "tip" shown in green that simultaneously pitches all of the blades. The tip is actuated by the rod shown in black. As seen in figure 12 a "carriage", shown in red, is attached to the rod and rotation of a power screw moves the rod forward and backward. There were no less than four iterations of this concept. The final design took great care in using a low amount of power, having an appropriate RPM around 15, having a high enough torque to pitch blades at a high wind speed, and lowering friction on all the moving contact points. This was achieved by using two guide rails and an acme threaded power screw. What is not pictured are limit switches which are going to be present to prevent overpitching one way or the other. To utilize a small DC motor a gearbox was constructed with 6 gear reductions for a decrease in RPM and an increase in torques of around 729:1.

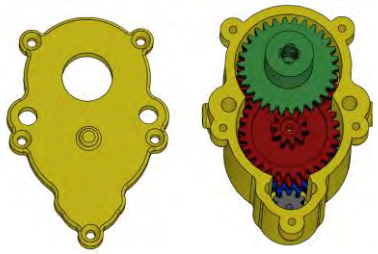

Figure 13: Gear box for pitching motor.

The combination of the mechanical pitch mechanism with the algorithm to maintain RPM resulted in an autonomously pitch-controlling wind turbine that both engineering teams should be proud of. Due to the complexity of the parts, 3D printing was utilized. The consideration was made for heat buildup in these parts. Since the PLA parts were constructed using 205°C thought was put into reducing friction in the carrier module that actuated the pitch-controlling rod. A set of thrust bearings proved to be sufficient during testing.

4.3 Tower

A simple static analysis showed that the tower needed to be of minimal strength. The tower was designed with very little thought as the forces that the turbine would undergo during construction and transportation would far exceed the forces during competition. The tower consisted of a 1-inch aluminum pipe with a 1/16" wall. The base will be mounted with a 3D printed bracket with enough clearance to accommodate 10mm wingnuts. A large diameter washer will help distribute the load from the force of the wingnut.

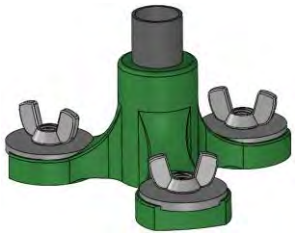

Figure 14: Foundation detail.

4.4 Nacelle

For a successful design, the placement of all the components within the nacelle was carefully planned. The axial flux motors would make up the bulk of the weight of the nacelle and the decision to split them around the yaw mechanism for weight distribution was made. From this initial decision, everything else was placed as needed. The yaw and pitch mechanisms were strategically placed where they were needed. Electrical components were placed to minimize the increase in the profile of the nacelle as much as possible.

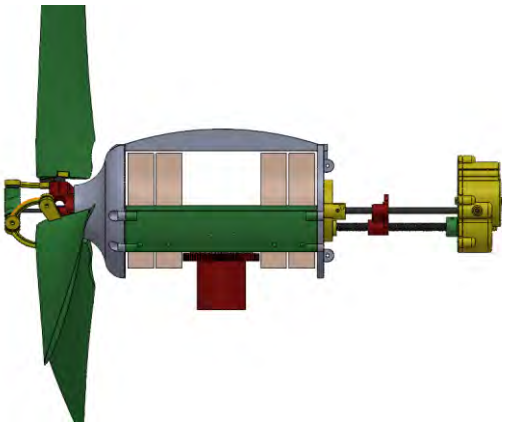

Figure 15: Overall assembly of the nacelle.

Structurally the nacelle was 3D printed due to the complex shape. Extra material was added as needed around the motors and the bearings which supported the main shaft. A thrust bearing was added to the front of the nacelle to ensure no axial load would be present throughout the rest of the wind turbine.

For the final cover plate, the EWET electrical engineering team made an observation that was too good to be a coincidence. The diameter of the nacelle and the electronics around the pitch control mechanism perfectly accommodated the shape of a 2-liter bottle. A few simple modifications had to be made for this non-optional feature to be implemented.

Not mentioned previously, the nacelle was also outfitted with a tachometer and a wind sensor. Cover plates will be added as necessary to pass safety inspections.

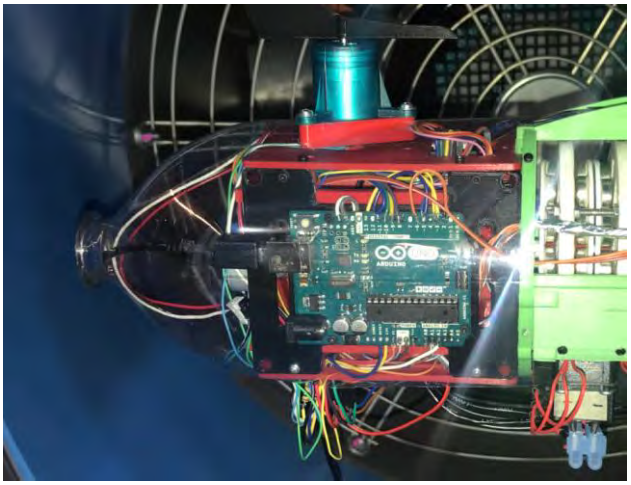

Figure 16: Ingenious adaptation of existing product.

4.5 Foundation

For the 2022 CWC competition, there is an offshore theme. To be consistent with this theme, one of the constraints was to implement a foundation, which would be installed into a water-filled tank that had 18cm of sand as a base. The foundation had to fit within a 25cm square and could penetrate the sand up to 15cm. Early on the decision was made to implement an auger-type attachment to utilize the sand as a means of structural support. The main forces considered when deciding how stable the foundation needed to be were the offset weight of the nacelle and the force from the wind on the cross-section of the turbine. The force from the offset weight of the nacelle was small and was overestimated as 44 Newtons (10 lbf). The force from the wind, F_{wind}, was calculated using the highest wind speed of 22 m/s and using formulation (12).

$$F_{wind} = \frac{1}{2}\rho_{air} A_{rotor} V_{\infty}^2 \quad (12)$$

Where ρ_{air} is the density of air (1.225 kg/m^3), A_{rotor} is the area of the rotor ($\pi r^2 \sim 0.16 m^2$), V_{∞} is the velocity of the wind -Force from the wind.

A force of 47 Newtons was calculated and would be present if the blades were a flat disc. The blades being used were of a high enough solidity that all of this force would be considered. Any difference would be considered as an additional factor of safety. A simple statics analysis using the moment arms associated with those forces was done. A downward force of 358 Newtons (80lbf) would be required in the center of the foundation to counteract the forces from the wind turbine operating at wind speeds of 22 m/s. A test was done on an auger with a 38 cm^2 cross section. It held 35 Newtons (8 lbf) before pulling out of the sand.

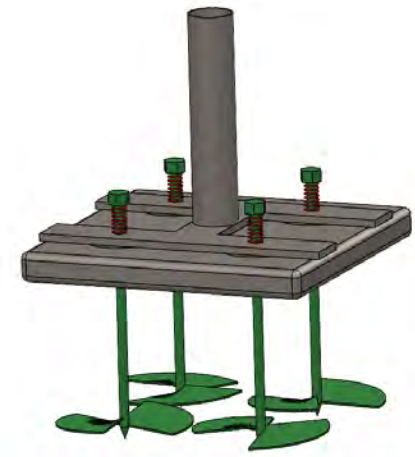

Figure 17: Foundation Assembly

Using the 358 Newton force required and the pull test of the auger, a foundation was designed using ~100 Newtons (23 lbf) of mass and four augers with a holding power of 93 Newtons each. The total theoretical holding force of the foundation will be 475 Newtons (106lbf). To ensure the augers have contact with the foundation, a compressed spring was used at the attachment of each auger. The compressed spring will also help with the vibrational load of an out-of-balance rotor.

With the initial forces on the foundation overestimated a factor of safety of 1.32 was achieved for the wind speed of 22 m/s. At the operational wind speed of 11 m/s, the same calculations produce a factor of safety of 70. Extra mass may still be considered for the final testing since the foundation is the lynchpin of the entire project.

4.6 Blades

The electrical and mechanical engineering teams decided to make an active pitch-controlled wind turbine that maintained 1200 RPM. The final blade design would have a twist that would be dependent on the wind speed and the speed of the blade. Looking at the scoring of the competition, the majority of the points available for the power curve generation task are for the wind speeds between 7m/s and 10m/s. The final twist of the blades was designed using 8m/s wind and a 1200 RPM rotor seen in Table 1. Using 1200 RPM as a baseline, the operational tip-speed ratios the turbine would undergo during testing would be 5.7 at 5m/s wind and 2.6 at 11 m/s wind. The blade design would be optimal were it designed in this range. These tip-speed ratios are low. Initially, a traditionally modeled blade (thicker at the base, thinner at the edge) was constructed. These blades failed to provide the torque required. A higher solidity blade was designed to produce more torque. This led to an airfoil that was linearly stretched as the radius increased. The thickness of the airfoil (Wortmann 83-W-108) was linearly stretched from 13mm at the mount to 5mm at the tip, providing a solid mounting point. For increased solidity, a wider blade was desired, so the chord was linearly stretched from 52.5mm at the base to 112.5mm at the tip, providing a much larger

cross-sectional area. Physical testing proved these blades operated sufficiently under a load and provided enough torque to the rotor. A bit of extra work was put into horizontally printing the blades for appropriate orientation of the stronger axis. Holes for set screws to balance the blades were put in.

Table 1: Blade Twist calculations based on radial velocity and 8 m/s wind speed.

Section	Radius (m)	Section Speed (m/s)	Wind Speed (m/s)	Blade Angle (°)
1	0.026	3.3	8.0	52.0
2	0.05	6.3	8.0	36.1
3	0.075	9.4	8.0	24.5
4	0.1	12.6	8.0	16.7
5	0.125	15.7	8.0	11.2
6	0.15	18.8	8.0	7.2
7	0.175	22.0	8.0	4.2
8	0.2	25.1	8.0	1.9
9	0.225	28.3	8.0	0.0

Given the additional time between the design report and the competition, additional adjustments may be done to the blades for a more optimal shape. The same RPM and wind speed specifications will be used.

5. Aerodynamic Design

The aerodynamic analysis for the final set of turbine blades for the 2022 CWC contest was done using QBlade. Due to the nature of the construction of the high-solidity blades, the original spline was modified at nine different points along the length of the blade. This resulted in the creation of nine different splines. For clarity, the even-numbered splines have been omitted.

The following aerodynamic analysis shows the process by which QBlade analyses spline, calculating polars, generating a theoretical lambda-Cp curve, and doing a structural analysis for a designed blade.

5.1 Aerodynamic Analysis

The non-traditional method of stretching and skewing an airfoil at different lengths resulted in the spline shapes shown in figure(M1). The spline that was modified was the Wortmann 83-W-108. The 5th spline is the closest to the original shape.

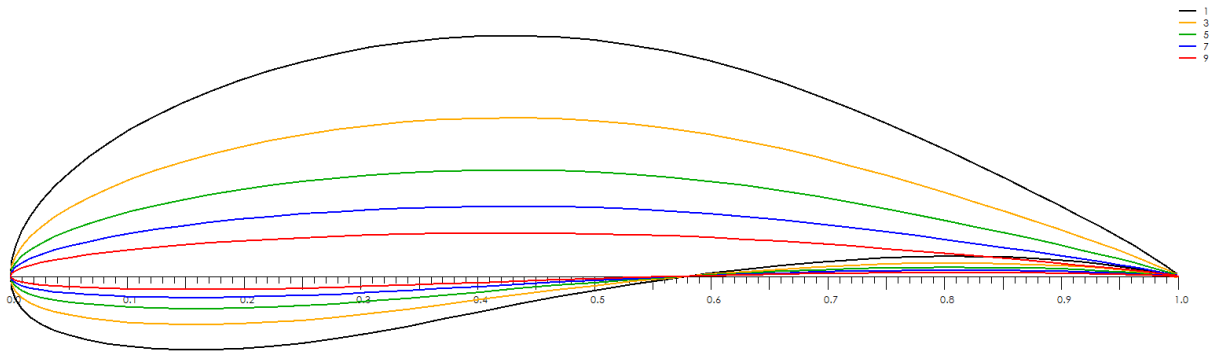

Figure 18: Odd-numbered splines used in the construction of the high solidity turbine blades.

QBlade has a built-in function to calculate the aerodynamic properties of any spline. Figure (19) shows a Cl/Cd (glide angle) vs Alpha (Angle of Attack). This will show the optimal angle of each spline shown in figure M1. Figure M3 shows the coefficient of lift for each spline should that angle be chosen.

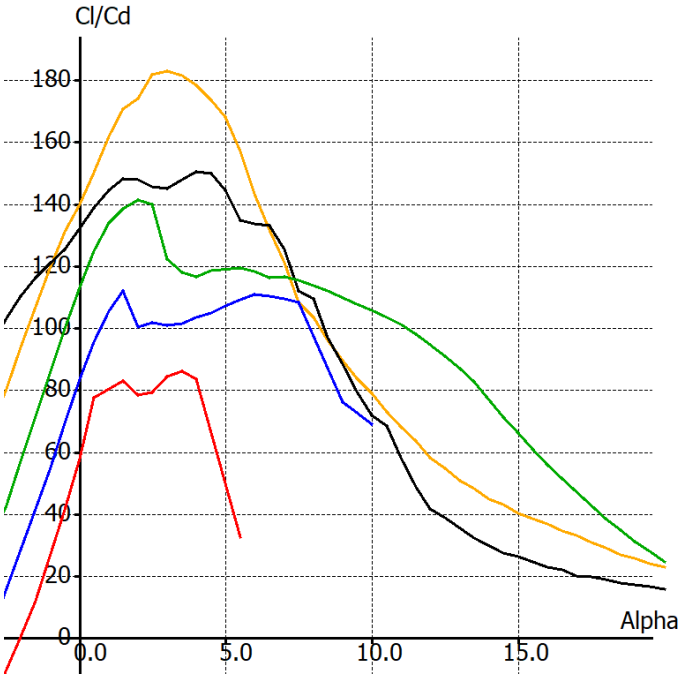

Figure 19: Cl/Cd (glide angle) vs. Alpha (angle of attack) for odd numbered splines.

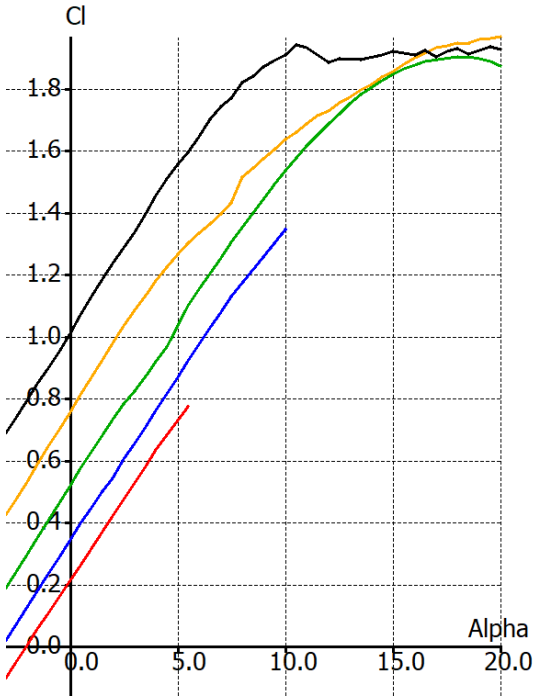

Figure 20: Coefficient of lift (Cl) vs Alpha for odd numbered splines.

5.2 CP-λ Curve

To help further analyze the blades QBlade allows the insertion of the geometry of the blade and will calculate a Lambda-Cp graph for a theoretical rotor, in this case, with three blades.

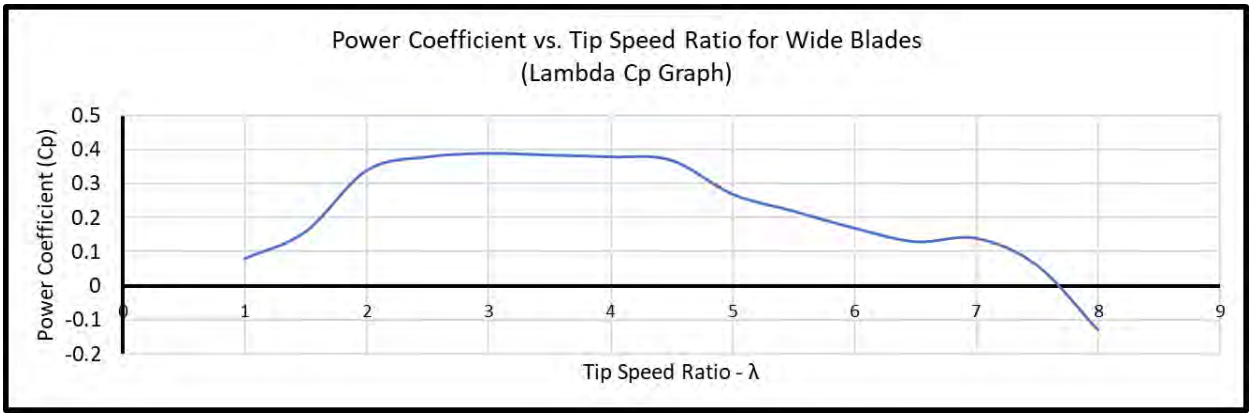

Figure 21: Lambda Cp curve for EWET rotor.

6. Experimental Verification

6.1 Blade Strength Test

An Instron pull test was done on the wind turbine blades. To calculate the force the blade must survive, the centrifugal force from a turbine blade operating at a speed of 2000 RPM. To determine the force that the blade must survive, formulation (13) is used.

$$F_{centrifugal} = m_{Blade}\omega^2 r_{c.m.} \quad (13)$$

Where m_{Blade} is the mass of the blade in kilograms, ω is the rotational speed in radians per second and $r_{c.m.}$ is the radius to center of mass of the blade. The result, $F_{centrifugal}$ is the centrifugal force.

Figure 22: Wide Blade in a pull-test.

Using the location of the center of mass from Solidworks, the weighed mass of 65 grams, and the high-end operational RPM of 2000, a force of 344 Newtons would be expected. The Instron pull test for one blade was done and broke the specimen at 2600 Newtons of force. This represents a factor of safety of 7.5. This expected centrifugal force was significantly larger than the normal and tangential aerodynamic forces that will be looked at later in the experimental analysis. With such a high factor of safety as is, it was not deemed necessary to analyze with all three forces.

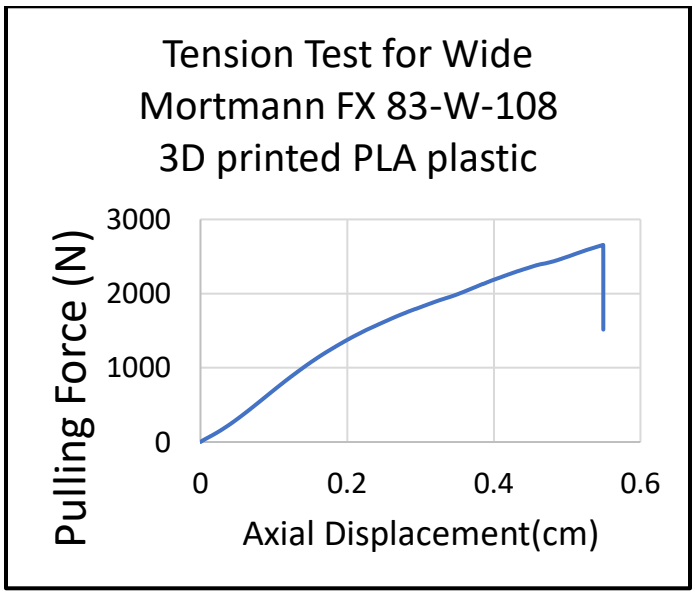

Figure 23: Pull-test graph Force vs. Displacement

Figure 24: Post Test Remains after 2600 N of force.

6.2 Aerodynamic force analysis

Using wind energy theory, a table of the normal and tangential forces that would be present on the blades at 11m/s. These forces would be analyzed using a moment arm and a study would be done on both the rotor hub and the blade to ensure that failure would not occur. This analysis was not done do the forces being two orders of magnitude smaller than the centrifugal force.

Using QBlade, a theoretical analysis was done on the blade to show where stress concentration would exist. Due to the nature of the calculations QBlade does, where a blade is described as a shell with an internal structure, this does not accurately predict the forces but can be used as a reference.

Table 2:Table of Normal and Tangential forces expected on the blade with 11 m/s wind and 1200 RPM

Normal (N)	Tangential (N)
0.14	0.19
0.54	0.43
1.51	0.77
3.14	1.10
3.70	0.90
3.96	0.66
5.17	0.58
5.74	0.39

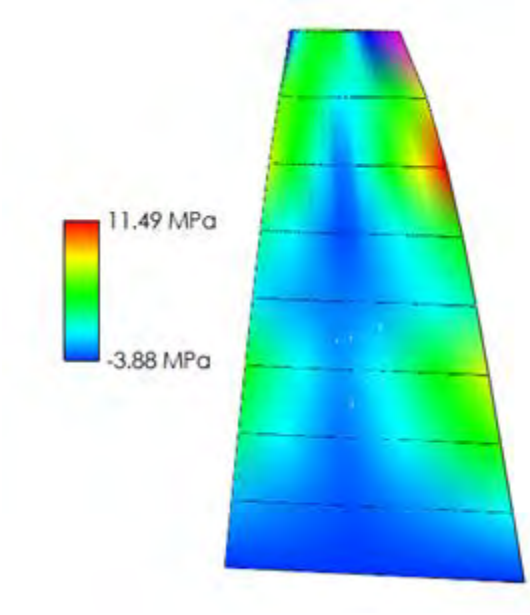

Figure 25: QBlade aerodynamic force analysis.

6.3 Power generation results

A test was done in the wind tunnel using the target RPM of 1200 and simulating a load on the turbine.

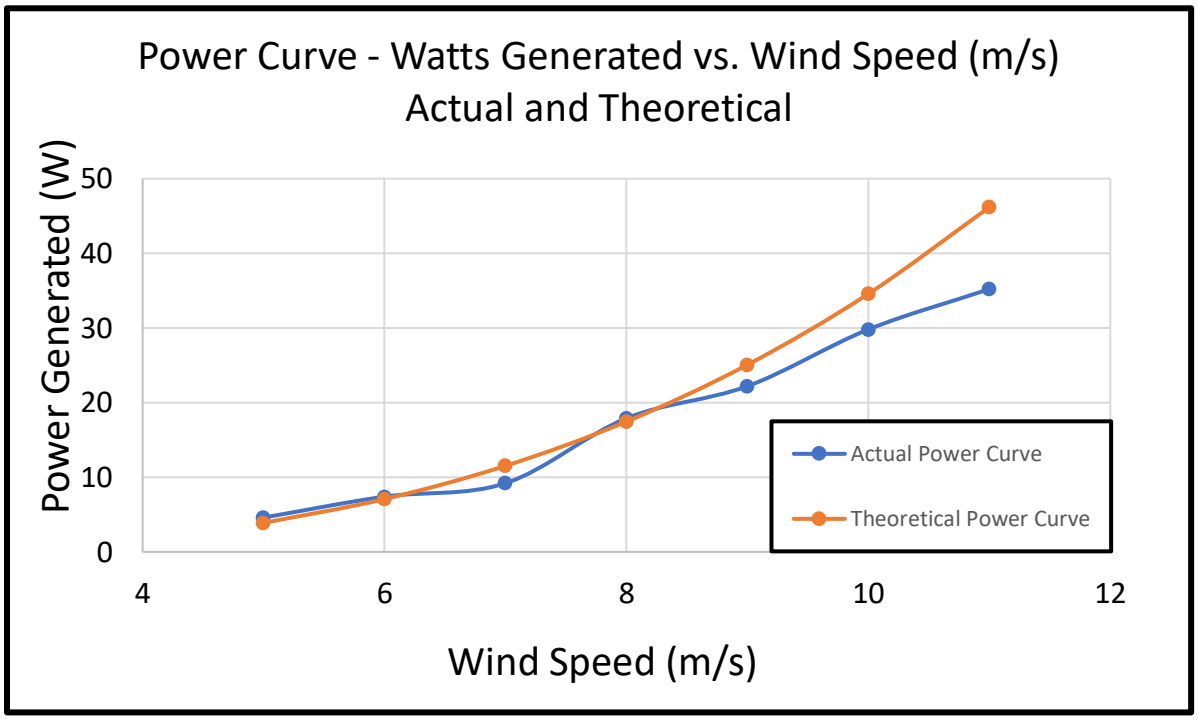

Figure 26: Power curve for the EWET wind turbine. Actual load measured in a wind tunnel. Theoretical load uses available power in the wind, Cp of 0.4, Mechanical efficiency of 0.9, and an electrical load of 0.5 Watts from electrical components.

6.4 Initial Generator Testing

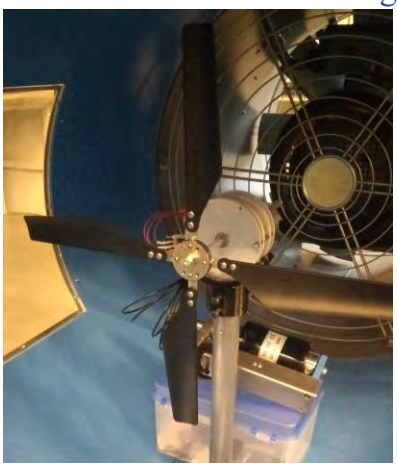

Figure 27: Wind tunnel testing of the single stack to determine KV rating.

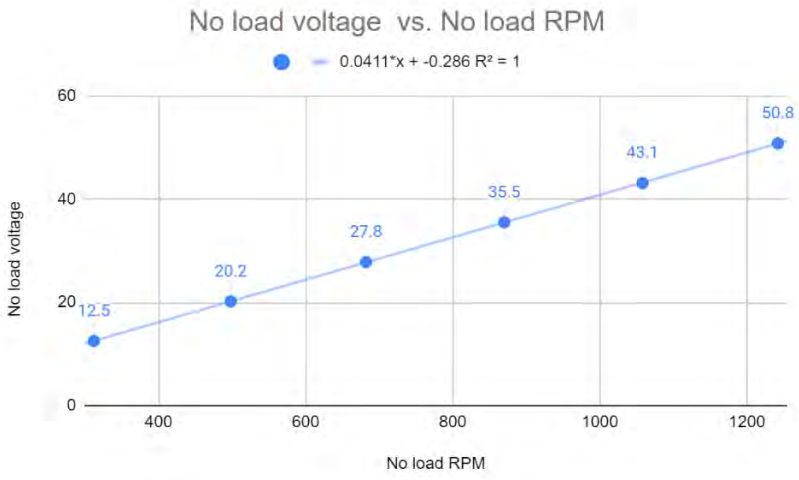

Figure 28: Graph of No-Load voltage vs. No-Load Rpm to determine KV rating.

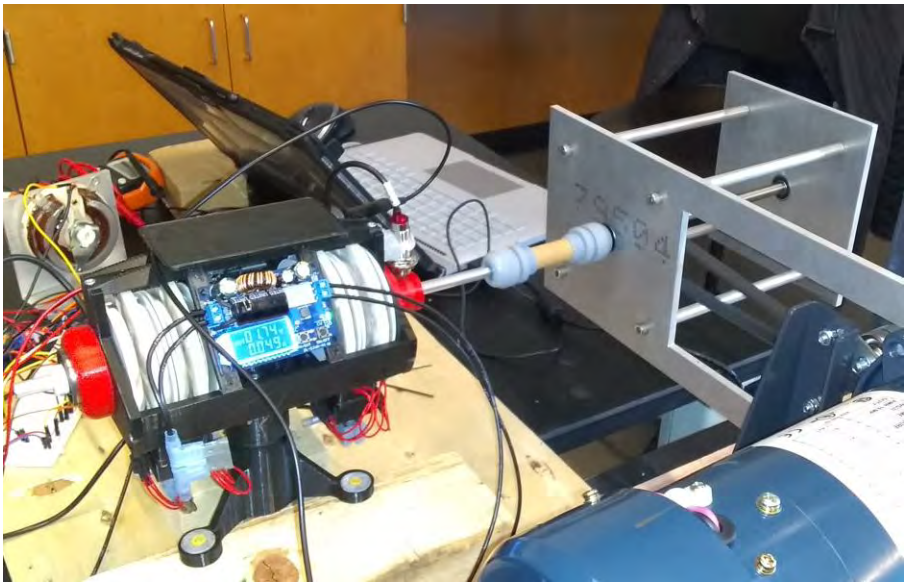

Figure 29: Dynamometer testing of the double tack setup.

7. Conclusion

Overall EWET's 2021-2022 design project was a success. We will bring a prototype to the competition in San Antonio ready to compete with the other teams. The mechanical engineering team created a physical wind turbine that would perform well within a wind tunnel. The electrical engineering team utilized the rotational energy and converted it into usable electricity to power the turbine and the load. We are excited to see what the other teams bring to the competition.

This was a great exercise in problem-solving, team cooperation, and communication.

References

Manwell, J.F., McGowan, J.G., Rogers, A.L. Wind Energy Explain – Theory, Design and Application, 2nd Edition. Wiley and Sons Publication 2009.